

ES2016-59252

UPSCALING, MANUFACTURING AND TEST OF A CENTRIFUGAL PARTICLE RECEIVER

Miriam Ebert

German Aerospace Center,
Institute of Solar Research
70569 Stuttgart, Germany
Telephone +49 711 6862 626
Telefax +49 711 6862 8032

miriam.ebert@dlr.de

Lars Amsbeck

German Aerospace Center,
Institute of Solar Research
70569 Stuttgart, Germany
Telephone +49 711 6862 306
Telefax +49 711 6862 8032

lars.amsbeck@dlr.de

Andrea Jensch

German Aerospace Center,
Institute of Solar Research
70569 Stuttgart, Germany
Telephone +49 711 6862 8081
Telefax +49 711 6862 8032

andrea.jensch@dlr.de

Johannes Hertel

German Aerospace Center,
Institute of Solar Research
70569 Stuttgart, Germany
Telephone +49 711 6862 786
Telefax +49 711 6862 8032

johannes.hertel@dlr.de

Jens Rheinländer

German Aerospace Center,
Institute of Solar Research
70569 Stuttgart, Germany
Telephone +49 711 6862 8169
Telefax +49 711 6862 8032

jens.rheinlaender@dlr.de

David Trebing

German Aerospace Center,
Institute of Solar Research
70569 Stuttgart, Germany
Telephone +49 711 6862 8172
Telefax +49 711 6862 8032

david.trebing@dlr.de

Ralf Uhlig

German Aerospace Center,
Institute of Solar Research
70569 Stuttgart, Germany
Telephone +49 711 6862 554
Telefax +49 711 6862 8032

ralf.uhlig@dlr.de

Reiner Buck

German Aerospace Center,
Institute of Solar Research
70569 Stuttgart, Germany
Telephone +49 711 6862 602
Telefax +49 711 6862 8032

reiner.buck@dlr.de

ABSTRACT

Previous successful tests and promising results of a Centrifugal Particle Receiver (CentRec) for high temperature solar applications has been achieved in a lab scale prototype with 7.5 kW_{th} [1, 2, 3]. In a next step this receiver technology is scaled up to higher thermal power for a future pilot plant.

This paper presents the optimization methodology of the design and technical solutions. It describes the manufacturing and assembly of the prototype and first tests and results of the commissioning including cold particle tests and prototype costs. Finally the paper gives an outlook on the planned further steps regarding hot lab tests and solar tests.

INTRODUCTION

One direct absorption receiver concept currently investigated at the DLR is the so-called Centrifugal Particle Receiver (CentRec) described in [1, 2, 4]. A schematic of the

principal design is given in FIGURE 1. Previous successful tests and promising results of this receiver have been achieved in a Proof-of-Concept (PoC) scale with 7.5 kW_{th} [1, 2, 3]. In a next step this receiver technology has been scaled up to higher thermal power for a future pilot plant.

The planned tests of the scaled up prototype are divided in several stages. For the first tests no solar tower test system is used but a test setup has been prepared at the University Stuttgart (see FIGURE 5). It consists of the receiver and necessary periphery, like particle storage and transportation system. 100 kW_{el} air cooled infrared heaters provide the needed thermal power for hot tests.

Manufacturing of the prototype, lab tests and first results are described in this paper.

DESIGN AND MANUFACTURING

Principal design of the centrifugal particle receiver:

The basic concept of the receiver shown in FIGURE 1 is a rotating cylinder with an inclination of the rotation axis towards horizontal. Particles enter into the receiver in the upper part at an inlet on the rotational axis and are accelerated by a feeding cone to the circumferential speed of the receiver. The particles form a particle film on the inner surface of the cylindrical absorber cavity. They move along the inner wall towards the outlet governed by gravity and centrifugal forces (see FIGURE 4). Concentrated sunlight enters through the aperture and heats up the particles through direct absorption. They leave the rotating receiver part at the lower end where a stationary collector ring catches all particles and conducts them to an outlet piping into the hot storage.

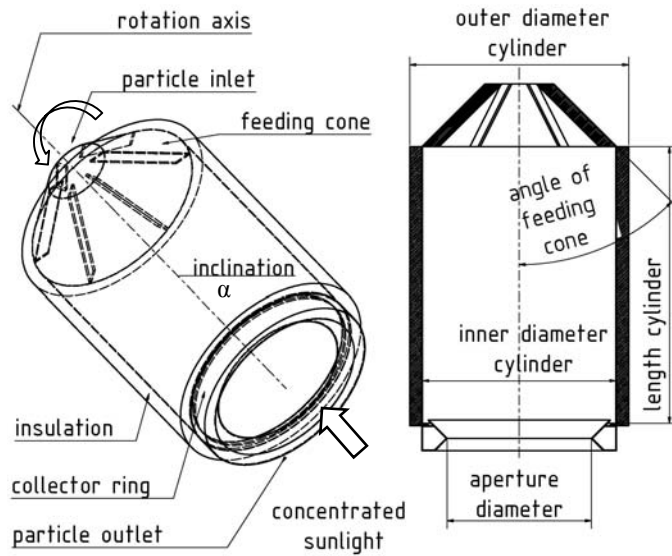


FIGURE 1: PRINCIPLE DESIGN OF THE CENTRIFUGAL PARTICLE RECEIVER

Tools and Methodology:

The optimization goal is a layout with minimal energy costs for a mature plant with costs expected after a couple of plants being built. The design point and annual performance is calculated with HFLCAL [5] as well as with SPRAY [6], a raytracing tool, to check the data.

The optimization described in [3] results in a configuration with eight towers and 2.5 MW_{th} power per 1 m²-CentRec to supply 6.2 MW_{th} of hot air at 750°C to a plasterboard plant from a 15 h particle storage. The tower height in the optimum configuration is 45 m. The maximum receiver power of 2.5 MW_{th} corresponds to a maximum particle mass flow per receiver of 3 kg/s at 200°C receiver inlet and 900°C outlet particle temperatures. These conditions are applied to design the scaled up receiver.

General design:

While it is assumed that geometric parameters like ratios given in Table 1 can be scaled up, the technical layout of components often needs major changes compared to the PoC, either because of size or manufacturing or costs. For the components of the prototype, concept studies are performed and evaluated regarding reliability, feasibility and cost.

The outer diameter of the receiver support structure should be smaller than the inner dimensions of a standard shipping container for both the prototype and the first demonstration plants. This ensures an easy and cheap transportation between place of manufacturing and site of operation. However, further scale up will probably require a modular setup of the receiver structure.

Therefore, the outer diameter of the rotating cylinder of 1.8 m is chosen. This, additionally considering 100 mm of nano-porous insulation, results in an aperture area of 1 m² with the geometric proportions of the PoC. The ratio between the inner diameter and the aperture diameter of the receiver and also the lengths of the receiver stayed similar to the values of the PoC. These are based on calculations of reflection losses of 3% with particles of 80% solar absorptivity or 1% losses at 90% absorptivity. The values are given in Table 1.

As particle motion is strongly dependent on the interaction of gravitational and centrifugal forces, the ratio between both forces determined for the PoC is the same for the prototype. To achieve the same centrifugal force as in the PoC the rotational speed n_{proto} results to 50 rpm with

$$n_{\text{proto}} = n_{\text{PoC}} \left(\frac{r_{\text{PoC}}}{r_{\text{Proto}}} \right)^{\frac{1}{2}}$$

and

$$n_{\text{PoC}} = 150 \text{ rpm}$$

$$r_{\text{PoC}} = 0.085 \text{ m}$$

$$r_{\text{Proto}} = 0.78 \text{ m}$$

Thus, the prototype is designed for a rotational speed of 80 rpm to ensure a safety margin.

Contrary to PoC design, this receiver is designed to allow for a thicker film. As PoC tests showed, it has been very difficult to obtain a homogenous velocity distribution with films of few particle diameters thickness. Thermal deformation of the inner receiver wall has been identified as the main problem, because it usually results in a variation of the isolation's radius, which in turn results in a different ratio between centrifugal and gravitational forces. Thus, a new design with a film of about 20 particle diameters thickness is used, to ensure a static base layer (see FIGURE 4) which can negate any thermal deformation and manufacturing faults.

With these basic geometric requirements and further design parameters given in Table 1 the detailed design of the components starts. After a first layout of the components static, dynamic and thermal finite element method simulations are conducted. Based on the stress analysis the final layout is realized and the component manufactured.

Detail design and manufacturing:

The main components of the prototype are as follows:

- structure of rotating part of receiver
- bearings
- drive
- feeding cone
- inner insulation
- component with damming edge to provide stationary basic particle layer (described in [2])
- collector ring
- support structure
- hot and cold particle storage, metering and transportation system for test setup
- infrared heaters for test setup
- measurement and data acquisition system

The outer structure is made of a welded tube of stainless austenitic steel reinforced with two flanges on both ends of the tube to increase the stiffness of the receiver. These flanges are used as running surface for the bearings and need to ensure the concentricity of the receiver. It supports a feeding cone, insulation, damming edge and particles during operation.

Table 1: Specifications of prototype

Aperture area and diameter	1 m ² , 1.13 m
Rotation axis inclination α	45°
Power of infrared heaters	100 kW _{el}
Thermal power	
Validation test setup	500 kW _{th}
Commercial setup	2,500 kW _{th}
Receiver outlet temperature	
Minimum	900°C
Design	1,000°C
Particle mass flow	3 kg/s
Ratio inner diameter cylinder / aperture diameter	>1.25
Ratio length cylinder / inner diameter cylinder	~1.5
Length of cylinder	2.3 m
Angle of feeding cone	45°
Rotational speed	Aprox. 50 rpm
Circumferential speed	3.8 m/s
Power of drive	7.5 kW
Outer dimensions support structure	2.3 m x 2.3 m
Used particles	Saint Gobain proppants 16/30 sintered Bauxite

Several bearing designs are investigated. The selected solution is based on bearing units made out of four ball bearing rolls each. The receiver is supported on the top end with a fixed bearing with four bearing units in axial direction and two in radial direction. Additionally, two spring loaded rolls are positioned opposite the radial units to ensure sufficient pressure on the radial bearings. The loose bearing consists of only two

radial bearing units and two spring loaded rolls. Thus, thermal expansion in axial and radial direction is possible. The position of the bearings is shown in FIGURE 2.

A chain drive is chosen as it is relatively robust against temperature, dust and vibration. It is cheaper and has less requirements regarding mechanical tolerances compared to, e.g., a belt drive chosen for the PoC. Due to the form-locking join and a normally slow and not sudden failure it has advantages regarding safety during solar operation.

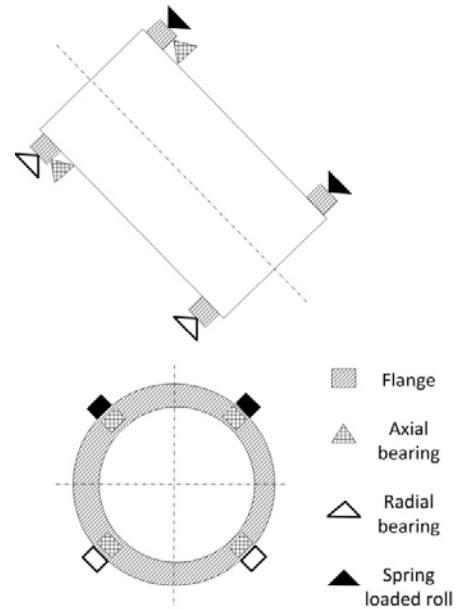


FIGURE 2: SCHEME OF POSITION OF BEARING



FIGURE 3: EXPLODED VIEW OF FEEDING CONE

The feeding cone shown in FIGURE 3 is made of heat-resistant steel, double-walled and equipped with 32 fins (instead of sixteen in the smaller PoC) between the walls. The angle of the feeding cone is selected with 45° the same as in the

PoC. A flat-angle or even planar design with less space required and easier manufacturing has been successfully tested in a smaller design and is planned to be used for the next design.

Inner insulation is required to reduce thermal losses and to protect the receiver structure against the high temperatures. It is made of microporous insulation material and mechanically protected and separated from the particle film with a thin inliner made of Inconel. This inliner is fixed on springs that allow an axial and radial expansion.

As described in [2] the homogeneity of the inner radius is of crucial importance. It would be very difficult and at least very expensive to machine the inliner of a bigger receiver to the desired tolerances. Thus, the idea is to provide the required geometry with a stationary base layer achieved by a high precision round damming edge on the outlet of the receiver.

The damming edge thickness is chosen to be 20 mm. Imperfections within the insulation are thus compensated by the base particle layer. This damming edge is realized by an overlapping, staggered arrangement of plates of non-oxide ceramic silicon carbide. It is concentrically mounted to the rotation axis of the receiver to achieve a homogenous particle film. Thus, an assembly jig is manufactured to ensure the high tolerances of roundness and precise alignment to the flanges of the bearing system. FIGURE 4 shows the principle of the function and a drawing of the component.

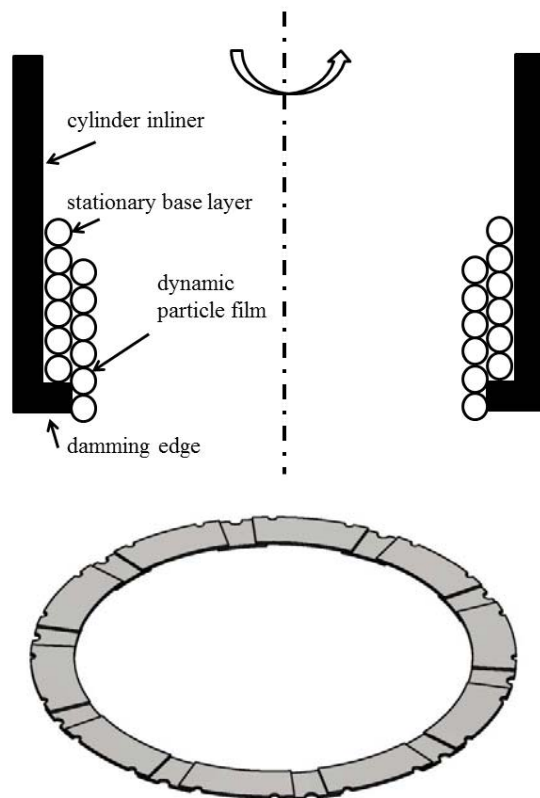


FIGURE 4: PRINCIPAL OF FUNCTION OF DAMMING EDGE AND DRAWING

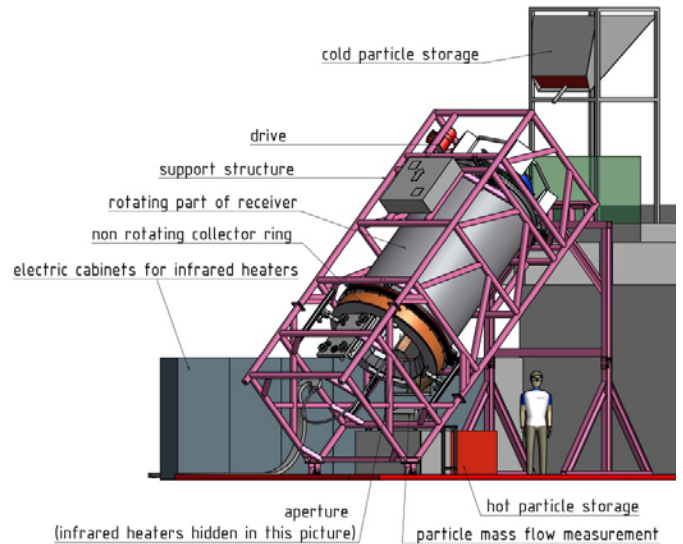


FIGURE 5: SET-UP OF THE CENTREC SCALED UP PROTOTYPE (A) SCHEMATIC DESIGN; (B) PHOTOGRAPH (WITHOUT COLLECTION RING)

The stationary collector ring should not block any incoming concentrated radiation. A polygon with 24 edges is chosen to approximate a rotationally symmetric design, to simplify manufacturing and inner insulation.

A support structure carries all components and is additionally used as transport structure. It is a welded framework of structural steel.

Ten infrared heaters of 10 kW_{el} each are assembled in two rows in a round arrangement. The space between them is insulated and the backside is actively cooled via air.

Using infrared heaters instead of concentrated solar radiation allows tests independent from meteorological conditions. Additionally, costs and effort for the operation of a heliostat field are saved. The heaters are positioned inside of the receiver to provide a flux distribution similar to the expected solar flux distribution in a solar field. Convection and radiation losses are minimized by an insulated aperture. Remaining conduction losses through the insulation can thus be determined.

A measurement and data acquisition system is incorporated into a Programmable Logic Controller. LabView [7] is used for managing data storage and as graphical user interface. All components are equipped with thermocouples. Additionally, rotational speed, particle mass flow and temperature at receiver in- and outlet are measured. The electric power of the heaters and dissipated energy of the cooling air of the infrared heaters are also recorded to be able to balance the system.

The whole set-up is shown in FIGURE 5.

TESTS AND RESULTS

Commissioning and tests are partly realized in parallel to comprehend as soon as possible how all components work. First, insulation and feeding cone are installed into the rotational part. Secondly, the receiver is mounted into the support structure with the bearing and is leveled. First manual rotational test are realized after that step. Next, chain drive and damming edge are installed and the whole assembly is positioned at an angle of 45°. Tests at up to 60 rpm are performed successfully. Vibrations due to unbalanced masses are observed but no need of balancing is seen at this point. Completing the installation of the particle system and the collector ring allow first particle tests. The first tests show a successful buildup of a stationary base layer on the damming edge. Up to now several tests are accomplished and first observations of the film are made.

In the following passages the film movement is described, within a cylindrical coordinate system with the tangential coordinate (azimuth Ω) originating at the bottom-most point within the receiver. Particle movement in the rotating receiver is governed by a superposition of gravitational force and centrifugal force. Obviously, rotational speed and radial distance from the rotational axis influence centrifugal force. Unless noted differently only situations with constant radius and rotational speed are discussed. Considering a cylinder with perfectly vertical rotation axis, centrifugal and gravitational forces stay at a constant alignment for every position (gravitational pull vertically; centrifugal force horizontally). If the rotational axis is not vertical, however, their alignment changes periodically. Ignoring the axial component, FIGURE 6 shows how both forces add up. Supposing an observer who travels with a particle, i.e. centrifugal force is stationary, it seems as if gravitation rotates. Gravitational force and centrifugal force act together in the lowest position ($\Omega = 0$) and

counteract each other in the highest position. At $\Omega = \pi/2$ and $\Omega = 3\pi/2$ gravitational force acts purely in tangential directions.

For the evaluation of the film movement a camera is mounted on the receiver inliner looking towards the aperture. FIGURE 9 shows the position and view of the camera and FIGURE 7 a picture taken from this camera with an empty receiver. While the collector is stationary, the camera rotates with the damming edge and the inliner. Particles exit the receiver through the gap between damming edge and collector.

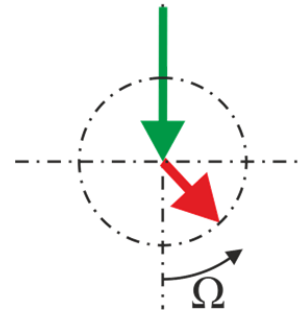


FIGURE 6: CENTRIFUGAL (GREEN) AND GRAVITATIONAL (RED) FORCES ON THE PARTICLES WITHIN THE RADIAL-TANGENTIAL PLANE

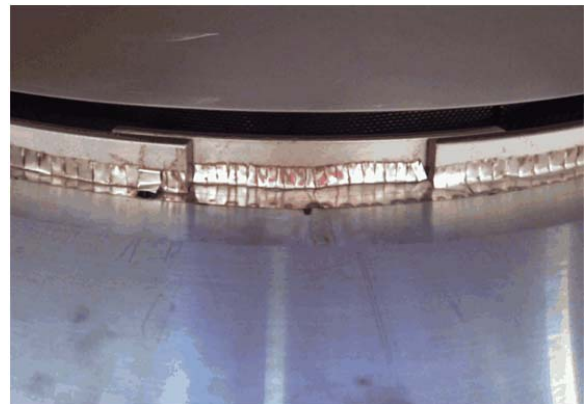


FIGURE 7: VIEW AT DAMMING EDGE, INLINER AND NON-ROTATING COLLECTOR RING

During operation of the receiver pictures of the particle film are taken and compared to each other. Between both frames in FIGURE 8 the receiver completed 26 revolutions at a relatively high rotational speed within the operational range. Several particles are marked in both frames and white dashed lines are added at fixed positions as references. Particles on the films' surface traverse slowly towards the aperture. It is assumed that with varying rotational speed the mass flow can be adjusted. However, as the mass flow measurement system is not yet operational this hypothesis is currently pending validation. At very low rotational speeds the film becomes unstable, as particles at the surface start to detach from the film and fall freely through the receiver.

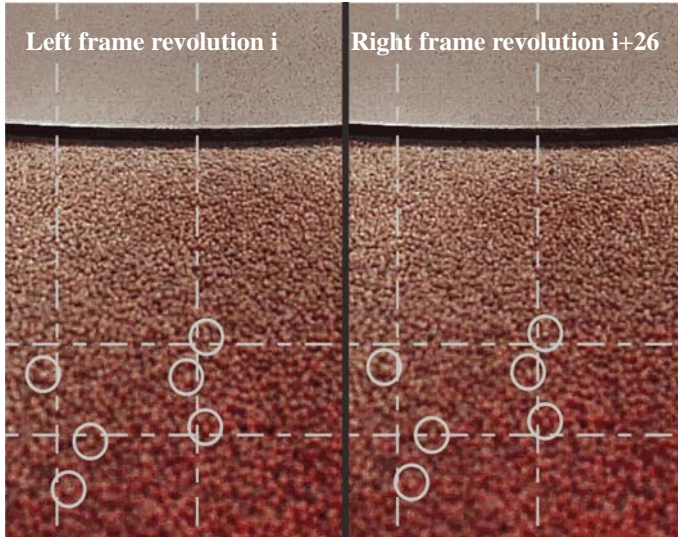


FIGURE 8: PARTICLE MOTION: WHITE, DASHED LINES SHOW FIXED POSITIONS; CIRCLE MARKS SPECIFIC PARTICLES; RIGHT FRAME IS TAKEN 26 REVOLUTIONS AFTER THE LEFT FRAME

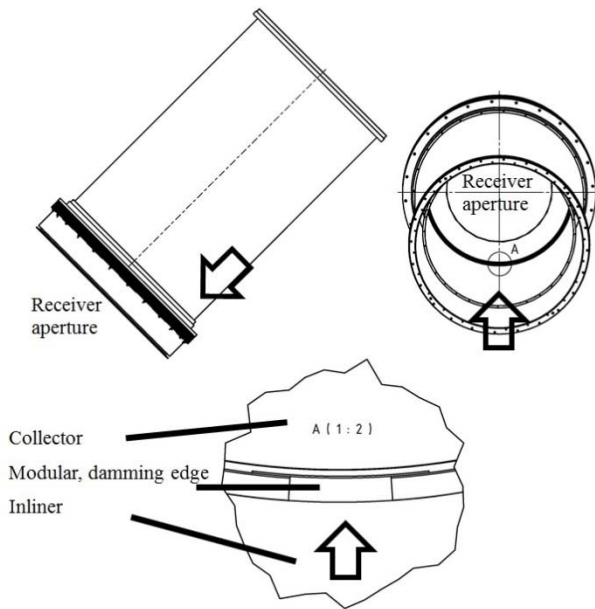


FIGURE 9: POSITION AND VIEW OF CAMERA (BLACK ARROW)

Granular films exhibit avalanches when certain criteria are met [8, 9]. Similar behavior within the CentRec can be observed. In FIGURE 10 a picture of an avalanche at a relatively low rotational speed is shown. From motion blur it is obvious that the avalanche enters the field of view from the bottom right with a significant tangential velocity. In fact, all avalanches exhibited the same zig-zag motion. As already discussed in FIGURE 6, gravitational pull rotates (from the

rotating observers point of view) thus resulting in a left-right pull on the film.

Additionally, it is observed that avalanches only exist in a distinct movement zone along the upper receiver mantle (see FIGURE 11). Outside of this zone, particles stand still relatively to the rotating wall. The zone width shows a dependence on the rotational speed. The lower the speed, the wider the movement zone and the bigger the step size in axial direction per receiver turn.

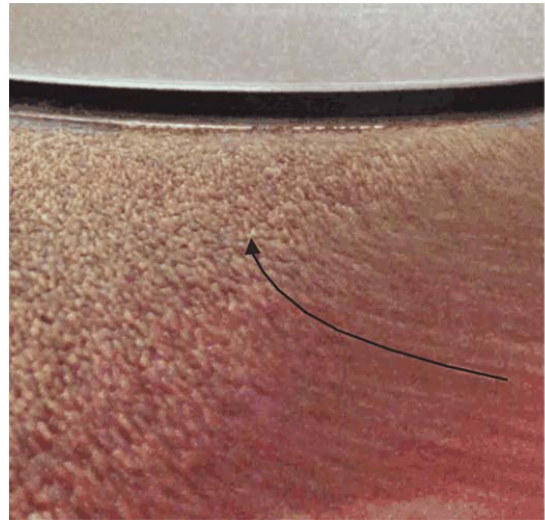


FIGURE 10: MOTION BLUR PICTURE OF AVALANCHE

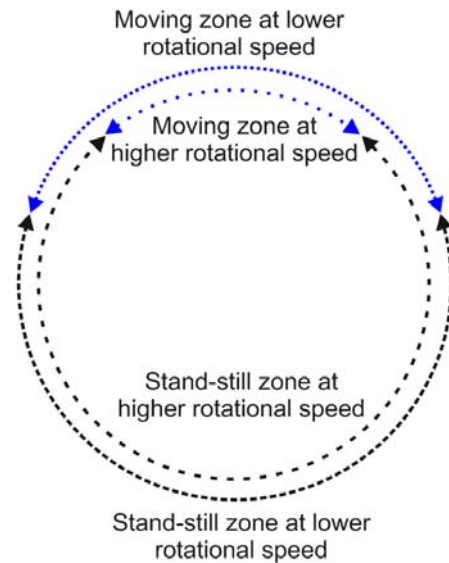


FIGURE 11: MOVEMENT ZONE AT DIFFERENT ROTATION SPEEDS

The authors assume that a precise control over the movement zones width can be used to design a particle movement scheme which achieves the desired outlet temperature under all load conditions. The more incoming radiation, the more particles can be heated and therefore the receiver has to rotate slower in order to widen the movement zone. To keep the particle film thickness at a constant value, mass flow into the receiver is adjusted to the outflow.

The specific hardware costs of the presented prototype are about 100 €/kW_{th} for 2.5 MW thermal power. By comparison, for instance, the molten salt receiver Solar Two costs were about 335 €/kW_{th} (216 €/kW_{th} * 55.5% cumulative rate of inflation) [10, 11] at a power level of 42 MW_{th}. Thus, the CentRec receiver shows very promising costs even at the prototype stage. Further improvements are possible regarding e.g. simplifications, a modular design of the receiver structure or purchasing commercially available bearings for higher number of units instead of an internal development.

CONCLUSIONS AND OUTLOOK

The present work shows the successful design, construction and cold-commissioning of a centrifugal particle receiver for 2.5 MW_{th} power. The scaled up design parameters from the PoC could be applied to the prototype. Changes on the design and new approaches for several components show good results after the first tests.

Hot commissioning is currently taking place. After the lab tests the prototype receiver unit will be installed in the solar tower power plant in Jülich (Solarthermisches Versuchs- und Demonstrationskraftwerk Jülich; STJ). In a first step solar tests with the prototype receiver and a particle transportation system are planned for 2016. In a second step system tests with hot storage and an air heat exchanger are planned in the solar tower in 2017/2018.

ACKNOWLEDGMENTS

This work was supported by the technology marketing of the German Aerospace Center (grant no. LRV 16/113) and the Helmholtz association (Helmholtz-Gemeinschaft Deutscher Forschungszentren e.V., HGF) validation-fond (Helmholtz-Validierungsfonds, HVF) (grant no. HVF-0028). The authors would also like to thank Birgit Gobereit and Tobias Prosinečki for their valuable contribution in this project.

REFERENCES

- [1] W. Wu, R. Uhlig, R. Buck, R. Pitz-Paal, "Numerical Simulation of a Centrifugal Particle Receiver for High-Temperature Concentrating Solar Applications", submitted to Numerical Heat Transfer, Part A: Applications, 2014
- [2] W. Wu, L. Amsbeck, R. Buck, R. Uhlig, R. Ritz-Paal, "Proof of concept test of a centrifugal particle receiver", Solarpaces 2013, Las Vegas, USA
- [3] L. Amsbeck, B. Behrendt, T. Prosin, R. Buck, "Particle tower system with direct absorption centrifugal receiver for high temperature process heat", Solarpaces 2014, Beijing, China

- [4] Wei Wu, "A centrifugal Particle Receiver for High-Temperature Solar Applications", PhD RWTH Aachen 2014, Logos Verlag Berlin 2015, ISBN 978-3-8325-3882-8

- [5] Schwarzbözl, P.: The User's Guide to HFLCAL. A Software Program for Heliostat Field Layout Calculation. Software Release Visual HFLCAL VH12. Köln 2009.

- [6] R. Buck. Spray Manual. DLR, 2010. 12, 79, 171

- [7] National Instruments Corporation: *LabView*. <http://www.ni.com>

- [8] Aranson, I. S. and L. S. Tsimring (2006). "Patterns and collective behavior in granular media: Theoretical concepts." Reviews of Modern Physics 78(2): 641-692

- [9] MiDi, G. D. R. (2004). "On dense granular flows." Eur Phys J E Soft Matter 14(4): 341-365

- [10] Reilly, H.E., and G.J. Kolb, 2001. "An Evaluation of Molten-Salt Power Towers Including the Results of the Solar Two Project," SAND2001-3674, Sandia National Laboratories

- [11] US Inflation Calculator, 2016, February 23rd, retrieved from <http://www.usinflationcalculator.com/>